

¹J. Owen, M. Browne, W. D. Knight, and C. Kittel, *Phys. Rev.* **102**, 1501 (1956); R. E. Behringer, *J. Phys. Chem. Solids* **2**, 209 (1957).

²K. Sugibuchi and E. Endo, *J. Phys. Chem. Solids* **25**, 1217 (1964); B. Caroli and A. Blandin, *J. Phys. Chem. Solids* **27**, 503 (1966).

³J. A. Seitchik, V. Jaccarino, and J. H. Wernick, *Phys. Rev.* **138**, A148 (1965).

⁴R. E. Walstedt, R. C. Sherwood, and J. H. Wernick, *J. Appl. Phys.* **39**, 555 (1968).

⁵M. A. Ruderman and C. Kittel, *Phys. Rev.* **96**, 99 (1954).

⁶T. Kasuya, *Progr. Theoret. Phys. (Kyoto)* **16**, 45 (1956).

⁷K. Yosida, *Phys. Rev.* **106**, 893 (1957).

⁸S. S. Dharmatti and R. Vijayaraghavan, *Current Sci. (India)* **15**, 449 (1964); C. Froidevaux, F. Gautier, and I. Weisman, in *Proceedings of the International Conference on Magnetism, Nottingham, England, 1964* (The Institute of Physics and The Physical Society, London, England, 1964), p. 390; I. D. Weisman and W. D. Knight, *Phys. Letters* **25A**, 546 (1967).

⁹D. Kaplan and E. L. Hahn, *J. Phys. Radium* **19**, 821 (1958).

¹⁰The *s*-band contribution is assumed to dominate here because of the large *s*-contact hyperfine field.

¹¹Small alloy buttons were prepared by inert electrode-arc melting of nominally 99.9+% Rh and 99.99% Co. They were homogenized by first cold working and then annealing in evacuated quartz ampoules for at least 24 h at 1000°C. The NMR powder samples were further annealed in evacuated quartz ampoules for 10 min at 750°C, followed by 24 h at 600°C. This treatment was sufficient to remove lattice strain resulting from grinding.

¹²M. Inoue and T. Moriya, *Progr. Theoret. Phys. (Kyoto)* **38**, 41 (1967).

¹³J. B. Ketterson, L. R. Windmiller, and S. Hörnfeldt, *Phys. Letters* **26A**, 115 (1968).

¹⁴J. R. Schrieffer and P. A. Wolff, *Phys. Rev.* **149**, 491 (1966).

¹⁵B. Caroli, *J. Phys. Chem. Solids* **28**, 1427 (1967).

¹⁶ $\langle S_z \rangle_{\text{Cu}}$ is the *s*-band polarization at a Cu site due to one Mn neighbor.

¹⁷J. Poitrenaud and J. M. Winter, *J. Phys. Chem. Solids* **25**, 123 (1964).

¹⁸N. Bloembergen and T. J. Rowland, *Phys. Rev.* **97**, 1679 (1955).

¹⁹A. Narath, A. T. Fromhold, and E. D. Jones, *Phys. Rev.* **144**, 428 (1966).

²⁰P. Lederer and D. L. Mills, *Solid State Commun.* **5**, 131 (1967).

STUDY OF THE JOSEPHSON PLASMA RESONANCE*

A. J. Dahm, A. Denenstien, T. F. Finnegan, D. N. Langenberg, and D. J. Scalapino
Department of Physics and Laboratory for Research on the Structure of Matter,
University of Pennsylvania, Philadelphia, Pennsylvania
(Received 14 March 1968)

We report direct observation of the plasma resonance in Josephson tunnel junctions. The properties of the plasma mode are found to agree quantitatively with theoretical predictions.

The electrodynamic of Josephson tunnel junctions has been the subject of numerous theoretical and experimental studies in recent years. One of the salient predictions of the theory, first noted by Josephson,¹ is the existence of a plasma-like mode of oscillation in such junctions. Although the experimental basis for our understanding of electrodynamic phenomena in junctions is rather extensive, this plasma mode has heretofore escaped direct experimental observation. We report here the first observation and study of the Josephson plasma resonance.

Before describing the experimental results, we would like to indicate how the plasma oscillation arises and to exhibit its dependence on various experimental parameters. We consider a tunnel junction consisting of two plane films of superconductor separated by an insulating barrier. Josephson has shown^{2,3} that in the absence

of externally applied magnetic and radio-frequency fields, the phenomenological equations describing the Josephson effects can be combined with Maxwell's equations to yield a nonlinear equation for the relative pair phase φ :

$$\nabla^2 \varphi - \bar{c}^{-2} (\partial^2 \varphi / \partial t^2) = \lambda_J^{-2} \sin \varphi, \quad (1)$$

where (in Gaussian units) $\bar{c} = c(l/\epsilon d)^{1/2}$ and $\lambda_J = (\hbar^2 c^2 / 8\pi j_1 e d)^{1/2}$. Here l is the barrier thickness, d is the sum of the barrier thickness and the penetration depths in the superconductors, j_1 is the Josephson current-density amplitude, and ϵ is the dielectric constant of the barrier material. In the case where φ undergoes small oscillations $\delta\varphi$ about φ_0 , Eq. (1) can be linearized by setting $\sin \varphi = \sin \varphi_0 + \delta\varphi \cos \varphi_0$. This yields the usual Meissner-effect equation plus the wave equation

$$\nabla^2 \delta\varphi + \frac{1}{\bar{c}^2} \frac{\partial^2 \delta\varphi}{\partial t^2} = \frac{\cos \varphi_0}{\lambda_J^2} \delta\varphi. \quad (2)$$

The solutions of this equation correspond to electromagnetic waves with dispersion relation $\omega^2 = \bar{c}^2 k^2 + \omega_p^2$, where $\omega_p^2 = \bar{c}^2 \cos\varphi_0 / \lambda_J^2 = 2ej_1 \cos\varphi_0 / \hbar C$; C is the junction capacitance per unit area. At $k=0$, the magnetic field associated with the mode is zero, the electric field and current are normal to the barrier plane (i.e., longitudinal), and there is a periodic exchange of energy between the electric field and the junction coupling energy. The mode thus has the characteristics of a plasma oscillation. It might be termed a "miniplasmon," since for typical junction parameters its frequency is of order 10^{10} Hz, much lower than typical plasma frequencies in metals. Note that the plasma frequency depends on $\cos\varphi_0$ and that the dc current in the junction depends on $\sin\varphi_0$, so that the plasma frequency can be controlled by varying the dc junction current. This is of prime importance in an experimental search for the plasma resonance.

The basic equation which describes the coupling of the plasma excitation to external fields and currents follows directly from Maxwell equation

$$\nabla \times \vec{H} = \frac{4\pi}{c} \vec{j} + \frac{\epsilon}{c} \frac{\partial \vec{E}}{\partial t} \quad (3)$$

for the fields in the barrier, and the Josephson constitutive relations for the current density perpendicular to the barrier:

$$j_{\perp} = j_1 \sin\varphi + \sigma E_{\perp},$$

$$\partial\varphi/\partial t = (2e\hbar/\hbar) E_{\perp}. \quad (4)$$

Here E_{\perp} is the electric field perpendicular to the barrier, σ is the quasiparticle conductivity of the junction, and the other parameters were defined above. In the pure plasma mode, E_{\perp} is uniform so that φ can be written as the sum of space-dependent and time-dependent parts,

$$\varphi = \varphi_0(x) + \delta\varphi(t). \quad (5)$$

Integrating Eq. (3) over a surface passing through the insulating barrier, converting the surface integral of $\nabla \times \vec{H}$ to a line integral of \vec{H} around the junction perimeter, and using the Josephson equations (4) to eliminate E_{\perp} in favor of $\delta\varphi(t)$, we obtain

$$\frac{\partial^2 \delta\varphi}{\partial t^2} + \frac{1}{RC} \frac{\partial \delta\varphi}{\partial t} + \omega_J^2 \langle \sin[\varphi_0(x) + \delta\varphi(t)] \rangle = \frac{2e}{\hbar C} I_{\text{ex}}. \quad (6)$$

Here R and C are the junction resistance (for quasiparticles) and capacitance $R = l/\sigma A$, $C = \epsilon A/4\pi l$; $\omega_J^2 = 2ej_1 A/\hbar C$; A is the junction area; and I_{ex} is the total externally supplied current, dc and/or rf. The angular brackets around $\sin[\varphi_0(x) + \delta\varphi]$ represent a spatial average over the junction.

In junctions with dimensions small compared with the Josephson penetration depth λ_J , $\varphi_0(x)$ varies linearly with applied dc magnetic field parallel to the barrier. In this case $\langle \sin\varphi_0(x) \rangle = \sin\varphi_0 |\sin\pi\Phi/\pi\Phi|$ and $\langle \cos\varphi_0(x) \rangle = \cos\varphi_0 |\sin\pi\Phi/\pi\Phi|$, where Φ is the flux contained in the junction measured in units of the flux quantum $hc/2e$. At finite temperatures, the Josephson current amplitude is reduced by the presence of thermally excited quasiparticles which interfere with the pair tunneling. For a junction composed of identical superconductors, j_1 varies with temperature as $[\Delta(T)/\Delta(0)] \tanh[\beta\Delta(T)/2]$, where $\Delta(T)$ is the energy gap parameter at temperature T .⁴

In the limit of small oscillations, Eq. (6) thus yields a plasma frequency

$$\omega_p^2 = \omega_J^2(0) \left[\frac{\Delta(T)}{\Delta(0)} \tanh\frac{1}{2}\beta\Delta(T) \right] \times \left| \frac{\sin\pi\Phi}{\pi\Phi} \right| \left[1 - \left(\frac{I_{\text{dc}}}{I_{\text{max}}} \right)^2 \right]^{1/2}. \quad (7)$$

The last term is $\cos\varphi_0$ expressed in terms of the ratio of the dc current driven through the junction to the critical dc current under the operating conditions.

From this discussion it is apparent that one should be able to detect the plasma resonance by probing a junction with a small microwave field at a suitable frequency and observing a resonant response at the plasma frequency. The dc current can be used to sweep the plasma frequency past the microwave frequency in the same manner as a magnetic field is used to sweep a resonant frequency in a conventional magnetic resonance experiment. It is desirable to perform the experiment in the small-signal regime, and this places rather stringent limitations on the power levels which can be used and the detection sensitivities which are required. The technique we have used involves applying a small microwave signal to a junction and detecting the second-harmonic signal generated by the junction nonlinearity. The separation of the input and output signals in frequency has advantages similar to

those obtained by separating input and output signals in space in conduction-electron-spin resonance experiments in metals by the transmission method. (This frequency-separation technique could be useful in the study of any system with an appropriate nonlinearity.) The second-harmonic output signal was detected using a phase-coherent detection system similar to that described by Lewis and Carver.⁵ This system was sensitive to both the phase and amplitude of the second-harmonic voltage. The output signal was proportional to the voltage. The system was capable of detecting 10^{-20} W of coherent second-harmonic signal with a 10-sec time constant. The detector output was plotted on an x - y recorder as a function of the dc junction current. In order to assure that all signals were observed with the junction operating in the zero-voltage dc Josephson mode, the recorder pen-lift input was driven by the amplified junction voltage so that the appearance of any nonzero voltage across the junction caused the recorder to cease writing.

Figure 1 shows a typical experimental recording. Two resonances appear, one at $\nu_p = \nu$ and one at $\nu_p = 2\nu$, where ν is the input frequency ($\nu_p = \omega_p/2\pi$). These can be understood as follows: In the small-signal limit, the current and voltage in the junction at frequency ν are related by a complex impedance $Z(\nu)$ which is that of a par-

allel LCR circuit with resonant frequency ν_p and $Q \equiv \omega_p RC$. At $I_{dc} = 0$, $\nu_p = \nu_J$ and $\nu_J > 2\nu$. As I_{dc} is increased, ν_p decreases as indicated by Eq. (7). When ν_p reaches 2ν , the amount of second-harmonic signal generated from the (essentially constant) input signal is resonantly enhanced as $Z(2\nu)$ passes through its resonance. When ν_p reaches ν , the amount of input signal at ν coupled into the junction increases because the coupling depends on $Z(\nu)$, and the second harmonic again peaks. We have calculated the phase and amplitude of the second-harmonic signal in the small-signal limit from Eq. (6), taking into account the effect of the junction impedance on the coupling into and out of the junction. The results are too cumbersome to present in detail here, but they are in accord with our observations. In particular, we note the following qualitative features: (1) The second-harmonic signal is proportional to I_{dc} and therefore reverses sign for negative I_{dc} . (2) Because the second-harmonic signal is proportional to the square of the fundamental signal, the resonance factor which peaks at $\nu_p = \nu$ appears squared. The second harmonic signal at $\nu_p = \nu$ is therefore larger than at $\nu_p = 2\nu$ by a factor of order Q , as observed. (3) For the same reason, the phase shift during passage through the resonance at $\nu_p = \nu$ is 2π , while that for the resonance at $\nu_p = 2\nu$ is π . This difference

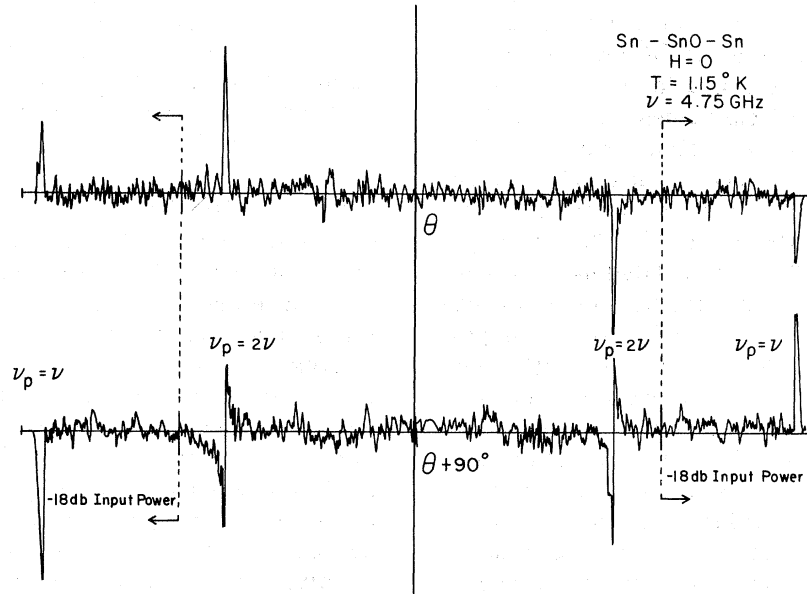


FIG. 1. Detected coherent second-harmonic voltage versus dc junction current for two different detector reference phases. The horizontal axis extends from $-I_{dc}^{max}$ to $+I_{dc}^{max}$. The input power was reduced by 18 dB to obtain the signals at $\nu_p = \nu$ in order to stay within the small-signal regime. Spurious second-harmonic signals were eliminated by using an output waveguide which was beyond cutoff at ν and by shielding and filtering elsewhere in the system.

is reflected in the different line shapes of the two resonances.

The Q of the observed resonances was typically several hundred at the lowest temperatures and decreased with increasing temperature in agreement with estimates of damping due to quasiparticle currents. A detailed study of the dependence of the Q on temperature and other experimental parameters is in progress and will be reported later.

Typical input power levels were 10^{-6} W and typical second-harmonic output powers were 10^{-18} to 10^{-17} W. Departure from the small-signal regime with increasing power was marked by a shift of the resonance toward lower I_{dc} accompanied by broadening and change of line shape. At still higher powers, hysteresis effects appeared. Quantitative data were taken well inside the small-signal regime.

In Fig. 2 are shown experimental values of ν_p^4 plotted versus the square of the normalized dc current for various temperatures. The linear dependence predicted by Eq. (7) is clearly observed. The data shown were obtained from a Sn-SnO-Sn thin-film tunnel junction (we have observed the resonance in several) with an area of 2.3×10^{-3} cm² and a maximum dc Josephson current of 4.1 mA at 1.15°K. This current was approximately 85% of the theoretical maximum current, which was taken to be equal to the observed sharp increase in the quasiparticle current at voltage $2\Delta/e$. The value of ν_J at 1.15°K obtained by extrapolating the data of Fig. 2 to zero dc current is 9.85 GHz. Theoretical values for comparison were calculated using a junction capacitance $C = \epsilon A/4\pi l$. ϵ/l was obtained by measuring \bar{c} from the junction self-resonant or Fiske modes; the result was $\bar{c} = 2.1 \times 10^9$ cm sec⁻¹. The quantity d in the formula for \bar{c} was calculated using a bulk penetration depth of 510 Å for tin. Using the observed value of I_1 we find $\nu_J = 8.8$ GHz; using the theoretical value we find $\nu_J = 9.6$ GHz. (Corrections for finite film thickness and finite mean free path could increase the effective penetration depth by as much as 25% and this would increase both these numbers by about half this amount.) The measured and calculated values of ν_J are in good quantitative agreement. The temperature dependence of ν_p is also in quantitative agreement with the predictions of Eq. (7) to within the experimental error. Resonances have been observed over the first two lobes of the magnetic-field diffraction pattern, in qualitative agreement with the expected field dependence.

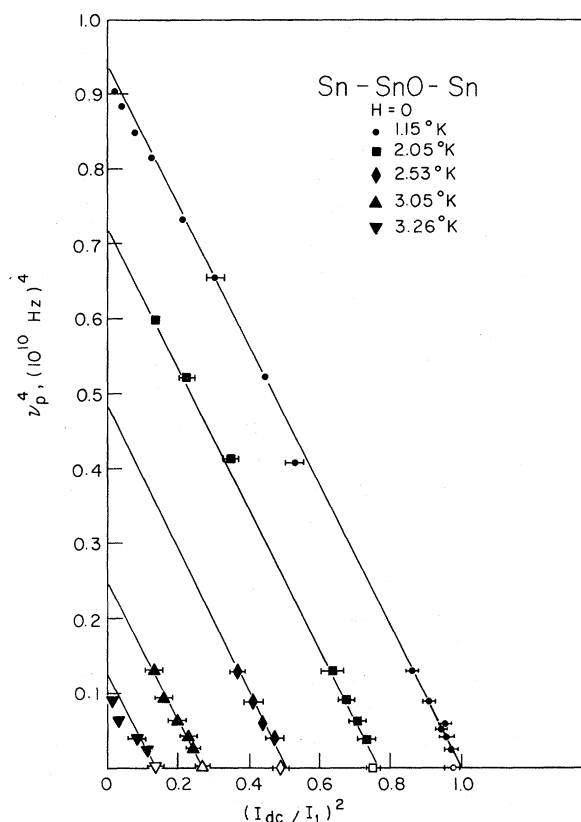


FIG. 2. ν_p^4 versus the square of the normalized dc junction current for several temperatures. The current normalization constant was determined from the best straight-line fit to the lowest-temperature data; the open data points are the maximum dc Josephson currents measured experimentally in the absence of applied rf voltage. The slopes of the higher temperature lines were taken equal to that of the low-temperature line, so that they represent a one-parameter fit.

We have also observed the plasma resonance by another method which is experimentally simpler, but more difficult to interpret quantitatively because the observed effects occur in the large-signal regime where the junction response is grossly nonlinear. Figure 3 is an oscilloscope plot of dc junction current versus the rf voltage applied to the junction. According to the simple theory of Shapiro,⁶ I_{dc}^{\max} is proportional to $J_0(2eV_{rf}/\hbar\omega)$, where J_0 is the Bessel function of order zero, so that the envelope of the current sweep in Fig. 3 should look like J_0 . In reality, a remarkable variety of singularities and hysteresis effects were observed. Note in particular the prominent notch in the envelope and the long, thin, dark region. The dark region is actually an inaccessible region of the current-voltage plane although currents all around it can

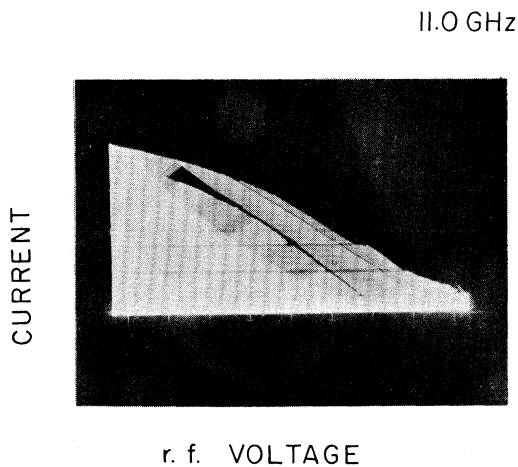


FIG. 3. Dc junction current versus input rf voltage. The trace was automatically blanked when the junction voltage was nonzero. The bright region thus represents accessible current values in the dc Josephson mode.

be reached. This behavior can be qualitatively understood in terms of resonant buildup of rf voltage in the junction at the plasma resonance with feedback-induced pulling of the plasma frequency leading to switching of the junction to a finite-voltage mode. We have been able to identify singularities corresponding to plasma resonances at the fundamental and fractional harmonics of the microwave frequency which are in good quantitative agreement with the results of the small-signal experiments.

The results reported here confirm the basic properties of the Josephson plasma mode predicted by theory and demonstrate a number of features which bear on other properties of Josephson junctions. Thermal excitation of the plasma mode gives rise to junction noise which can ultimately destroy the phase locking. We observe the characteristic shift to lower frequencies of the spectral density associated with this excitation as T approaches T_c . The effect of thermally excited plasmons thus becomes an increasingly important source of low-frequency phase fluctuations as the transition temperature is approached. We also believe that the plasma

mode plays a major role in the behavior of junctions as radiation detectors in the millimeter and submillimeter region. Our experimental results and calculations based on Eq. (6) show that the suppression of the dc critical current by rf radiation exhibits sharp resonances associated with the plasma mode, a possibility which has been noted by Anderson⁷ in connection with experiments by Grimes, Richards, and Shapiro.⁸ We estimate that the plasma mode in typical point-contact Josephson junctions occurs at frequencies of order 10^{12} Hz because of the small junction capacitance. Just as in the present experiments, this frequency is reduced as the dc current through the point contact is increased towards its critical value. Some of the unexplained structure in the frequency dependence of the submillimeter response of junctions reported by Grimes, Richards, and Shapiro may very well be associated with plasma resonances. The sensitivity of the plasma mode to external fields and currents demonstrated in the present experiments suggests a number of interesting applications to Josephson junction radiation detectors.

We wish to thank L. K. Anderson for a timely equipment loan.

*Research supported by the National Science Foundation and the Advanced Research Projects Agency.

¹B. D. Josephson, *Rev. Mod. Phys.* **36**, 216 (1964).

²B. D. Josephson, *Advan. Theoret. Phys.* **14**, 419 (1965).

³B. D. Josephson, in *Quantum Fluids*, edited by D. F. Brewer (North-Holland Publishing Company, Amsterdam, The Netherlands, 1966).

⁴V. Ambegaokar and A. Baratoff, *Phys. Rev. Letters* **10**, 486 (1963), and **11**, 104(E) (1963).

⁵Richard E. Lewis and Thomas R. Carver, *Phys. Rev.* **155**, 309 (1967).

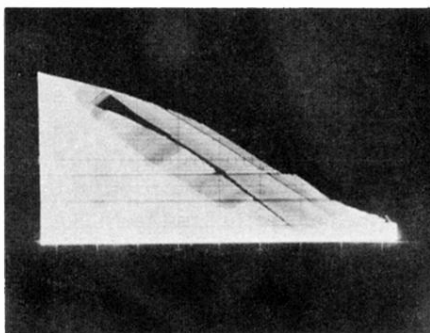
⁶S. Shapiro, *Phys. Rev. Letters*, **11**, 80 (1963); S. Shapiro, A. R. Janus, and S. Holly, *Rev. Mod. Phys.* **36**, 223 (1964).

⁷P. W. Anderson, in *Progress in Low-Temperature Physics*, edited by C. J. Gorter (North-Holland Publishing Company, Amsterdam, The Netherlands, 1967), Vol. V.

⁸C. C. Grimes, P. L. Richards, and S. Shapiro, *Phys. Rev. Letters* **17**, 431 (1966), and to be published.

11.0 GHz

CURRENT



r. f. VOLTAGE

FIG. 3. Dc junction current versus input rf voltage. The trace was automatically blanked when the junction voltage was nonzero. The bright region thus represents accessible current values in the dc Josephson mode.